Dalton Transactions

Accepted Manuscript

ROYAL SOCIETY OF CHEMISTRY

www.rsc.org/dalton

Journal Name

RSCPublishing

ARTICLE

New Insights into the Chemistry of Di- and Trimetallic Iron Dithiolene Derivatives. Structural, Mössbauer, Magnetic, Electrochemical and Theoretical Studies

Sonia Bruña,[a] Isabel Cuadrado,[a] Esther Delgado,*[,a] Carlos J. Gómez-García,[b] Diego Hernández,[a] Elisa Hernández,[a] Rosa Llusar,[c] Avelino Martín,[d] Nieves Menéndez,[e] Victor Polo,[f,g] and Félix Zamora[a]

estherCite this: DOI: 10.1039/x0xx00000x

Received 00th January 2012,
Accepted 00th January 2012

DOI: 10.1039/x0xx00000x

www.rsc.org/

Reaction of $Fe_3(CO)_{12}$ with the 1,2-dithiolene $HSC_6H_2Cl_2SH$ affords a mixture of complexes $[Fe_2(CO)_6(\mu\text{-}SC_6H_2Cl_2S)]$ **1**, $[Fe_2(SC_6H_2Cl_2S)_4]$ **2** and $[Fe_3(CO)_7(\mu_3\text{-}SC_6H_2Cl_2S)_2]$ **3**. In the course of the reaction the trimetallic cluster **3** is first formed and then, converted into the known dinuclear compound **1** to afford finally, the neutral diiron tetrakis(dithiolato) derivative **2**. Compounds **2** and **3** have been studied by Mössbauer spectroscopy, X-ray crystallography and theoretical calculations. In compound **2** the metal atoms are in an intermediate–spin Fe^{III} state (S_{Fe} = 3/2) and each metal is bonded to a bridging dithiolene ligand and a non-bridging thienyl radical (S = 1/2). Magnetic measurements show a strong antiferromagnetic coupling in complex **2**. Cyclic voltammetry experiments show that the mixed valence trinuclear cluster **3** undergoes a fully reversible one electron reduction. Additionally, compound **3** behaves as electrocatalyst in the reduction process of protons to hydrogen.

Introduction

Transition metal complexes with 1,2-dithiolenes is a subject of high research interest as a consequence of their rich redox chemistry, versatility in the coordination modes, biological function, as well as their well-known magnetic and electrical conducting properties.[1] Ott *et al*[2] have described the formation of the di-iron derivatives $[Fe_2(CO)_6(\mu\text{-}SRS)]$ (R = C_6H_4 or $C_6H_2Cl_2$) as the sole compound from the thermal reaction of $Fe_3(CO)_{12}$ with the corresponding dithiolene. On the other hand, Huttner *et al*[3] have reported analogous reactions but using aliphatic dithiols, such as $HSCH_2CH_2SH$ or $HSCH_2CH_2CH_2SH$, in which a trinuclear cluster $[Fe_3(CO)_7(\mu\text{-}SRS)_2]$ is isolated together with the dinuclear species $[Fe_2(CO)_6(\mu\text{-}SRS)]$. To our knowledge these two triiron clusters and the analogous complex $[Ru_3(CO)_7(\mu\text{-}SCH_2CH_2S)_2]$[4] are the only examples reported on mixed valence heptacarbonyl trinuclear derivatives of group 8 containing dithiolato ligands. Additionally, the close related compound $[Fe_3(CO)_7(\mu_3\text{-}SC_6H_4N{=}N)_2]$ containing a diazenylbenzenethiolato group is also known.[5]

Compounds $[Fe_2(CO)_4L_2(\mu\text{-}SRS)]$ (L= CO, phosphine or CN^-; R= aliphatic or aromatic groups) are being studied as valuable models of the active site of the [FeFe] hydrogenase.[6] Additionally, the role of the mixed valence clusters $[Fe_3(CO)_7(\mu\text{-}SCH_2CH_2S)_2]$[7] and $[Fe_4\{MeC(CH_2S)_3\}_2(CO)_8]$[8] as electrocatalysts for the reduction of the protons to hydrogen have also been explored.

We have recently obtained a one dimensional coordination polymer of an iron dithiolene derivative, $\{[K_2(\mu\text{-}H_2O)_2(thf)_4][Fe_2(SC_6H_2Cl_2S)_4]\}_n$, with rather unexpected physical properties: *i*) it is the first coordination polymer containing an "s" group metal as a bridging building block showing electrical conductivity; *ii*) it represents the first example of a coordination polymer showing two electrical transition phases and, *iii*) it shows electrical bi-stability.[9] This coordination polymer is isolated from the reaction of $[Fe_2(CO)_6(\mu\text{-}SC_6H_2Cl_2S)]$ with $HSC_6H_2Cl_2SH$, in the presence of K_2CO_3. These interesting results have prompted us to extend our work to evaluate this reaction under similar experimental conditions but in the absence of K_2CO_3. This slight synthetic change has led to the formation of the neutral diiron^{III,III} tetrakis(dithiolato) derivative $[Fe_2(SC_6H_2Cl_2S)_4]$ **2**. In addition, the synthesis of the mixed valence cluster $[Fe_3(CO)_7(\mu_3\text{-}SC_6H_2Cl_2S)_2]$ **3**, is also described. The redox properties of $[Fe_3(CO)_7(\mu_3\text{-}SC_6H_2Cl_2S)_2]$ **3** have been examined by electrochemical techniques.

Results and discussion

Synthesis and Characterization of Complexes 2 and 3

A toluene solution of compound $[Fe_2(CO)_6(\mu\text{-}SC_6H_2Cl_2S)]$ **1** and the 1,2-dithiolene $HSC_6H_2Cl_2SH$ in 1:3 ratio, was refluxed under stirring for 24 h (Scheme 1). The solid formed was filtered and crystallized in acetone/n-hexane (1:2) at –20 ºC to yield the purple compound **2**.

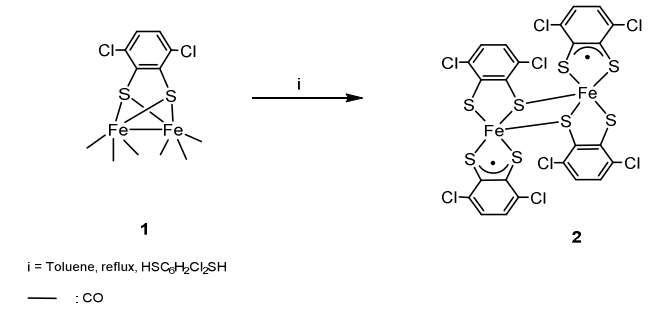

Scheme 1

The microanalytical data and the presence of the parent ion in the mass spectrum suggested the formulation of complex **2** as $[Fe_2(SC_6H_2Cl_2S)_4]$. The molecular structure of this neutral compound was confirmed by single crystal X-ray diffraction. The metal oxidation states were assigned based on Mössbauer studies and DFT calculations (*vide infra*). The high insolubility of compound **2** in the most common organic solvents, together with the experimental observation that a dark residue was always retained on the top of the column chromatographic used to purify compound **1**, obtained from $Fe_3(CO)_{12}$ with $HSC_6H_2Cl_2SH$,[2] prompted us to reinvestigate if compound **2** is also formed in this reaction. Thus, after keeping the mixture stirred under refluxing toluene during 45 min, the solvent was removed and the residue purified on silica gel. A carefully performed chromatographic column allowed us to separate three bands: $[Fe_2(CO)_6(\mu\text{-}SC_6H_2Cl_2S)]$ **1**, and two new bands corresponding to $[Fe_2(SC_6H_2Cl_2S)_4]$ **2** and $[Fe_3(CO)_7(\mu_3\text{-}SC_6H_2Cl_2S)_2]$ **3** (Scheme 2).

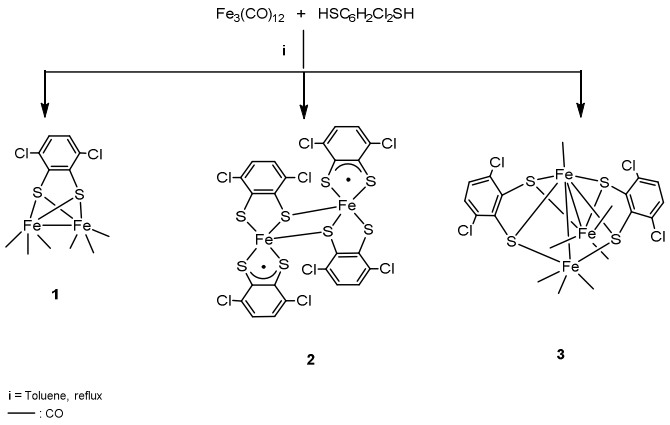

Scheme 2

The structure of the mixed valence cluster **3** was confirmed by single crystal X-ray diffraction. We have observed that longer reaction times and larger amounts of dithiolene, in comparison to the procedure described before, improve the yields of the new derivatives **2** (17.3% yield) and **3** (6.4% yield) (see experimental section). We have also studied the reaction between $Fe_3(CO)_{12}$ and $HSC_6H_2Cl_2SH$ in the presence of $ONMe_3$. In this case, a remarkable increase in the yield of compound $[Fe_2(SC_6H_2Cl_2S)_4]$ **2** (40 % yield) is observed while only trace amounts of $[Fe_3(CO)_7(\mu_3\text{-}SC_6H_2Cl_2S)_2]$ **3** obtained.

In order to know whether there is any relationship between compounds **1–3**, a mixture of **3** and $HSC_6H_2Cl_2SH$, was left in refluxing toluene for 3 h. Afterwards, compound **1** was isolated as the major product together with traces of **2**. This result in addition to the conversion of the dinuclear carbonyl derivative **1** in the neutral compound **2**, as commented before, suggests that the cluster $[Fe_3(CO)_7(\mu_3\text{-}SC_6H_2Cl_2S)_2]$ **3** is the first compound formed in the reaction of $Fe_3(CO)_{12}$ with $HSC_6H_2Cl_2SH$. This process implies the substitution of CO groups by dithiolato ligands and the cleavage of one Fe–Fe bond in the precursor $Fe_3(CO)_{12}$. In a second step, probably the rupture of Fe-Fe and Fe-S bonds as well as formation of a new Fe-Fe bond in **3** would yield to compound $[Fe_2(CO)_6(\mu\text{-}SC_6H_2Cl_2S)]$ **1** and, finally, total substitution of carbonyls by dithiolato in compound **1**, generates $[Fe_2(SC_6H_2Cl_2S)_4]$ **2** (Scheme 3).

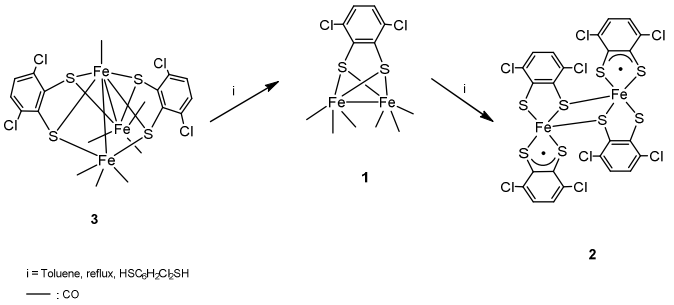

Scheme 3

The IR spectrum of compound **3** exhibits υCO bands at 2077 (m), 2054 (vs), 2022 (w), 2016 (s), 1999 (vw) and 1977 (s) cm^{-1} corresponding to terminal carbonyl ligands. The pattern of the IR spectrum of **3** is rather similar to that reported for $[Fe_3(CO)_7(\mu\text{-}SRS)_2]$ (R= CH_2CH_2 and $CH_2CH_2CH_2$).[3] In the latter compounds an additional band corresponding to the presence of a semi-bridging CO ligand was also observed but this feature is not observed in the spectrum of **3**. Moreover, a resonance at δ 7.10 ppm, for the protons assigned to the $C_6H_2Cl_2$ groups is shown in its ^1H NMR spectrum. Finally, the mass spectrum of **3** shows the parent ion and other ions assigned to successive loss of CO's groups.

X-ray Diffraction, Mössbauer, Magnetic and Theoretical studies of Compound 2

The molecular structure of complex **2** has been determined by the neutral diferric complex. Selected bond distances and angles are given as figure caption (Figure 1). The $[Fe(SC_6H_2Cl_2S)_2]$ moiety in complex **2** presents an iron centre which is S,S-bond to one dithiolato and one thienyl ligands. Additionally, each FeL_2 entity acts as μ-sulfur bridging two metal centres leading to a distorted 4+1 square based pyramidal geometry around the iron atoms.

Certainly, from ligand bond distances analysis there is some indication that the terminal non-bridging dithiolato ligands are in their oxidized form. An average of 1.758(2) Å for the [S(4)-C(12)] and [S(3)-C(7)] distances as well as a bond length of 1.43(1) Å for C(7)-C(12) are observed for this terminal non-bridging thienyl ligand, whereas a shortest C-C bond length of 1.40(1) Å [C(1)-C(2)] and an average of 1.77(2) Å for the S-C bond distances are found for the terminal bridging dithiolato group. These data agree with those previously reported species $[Fe^{III}_2\{S_2C_2(C_6H_4\text{-}p\text{-}CH_3)_2\}_4]$[10] and $[Fe^{III}_2\{S_2C_2(C_6H_4\text{-}p\text{-}OCH_3)_2\}_4]$.[11] To our knowledge, the two former compounds and $[Fe_2(SC_6H_2Cl_2S)_4]$ **2** are the only examples on neutral $Fe^{III}Fe^{III}$ tetrakis(dithiolato) dimers which crystal structures have been reported.

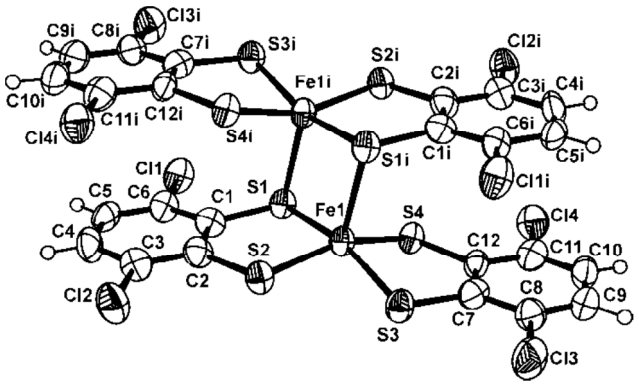

Figure 1. View of the molecular structure of **2**. Selected bond lengths (Å) and angles (deg):C1-C2 1.40(1), C1-S1 1.787(8), C2-S2 1.745(8), C7-C12 1.43(1), C7-S3 1.757(8), C12-S4 1.760(7), S1-Fe1 2.225(2), S1-Fe1^{i} 2.494(2), S2-Fe1 2.244(2), S3-Fe1 2.194(2), S4-Fe1 2.244(2), S1-Fe1-S2 89.19(8), S3-Fe1-S4 88.88(8), S2-Fe1-S3 87.56(8), S1-Fe1-S4 87.93(8), S1-Fe1-S1^{i} 99.45(7), S2-Fe1-S1^{i} 100.55(8), S3-Fe1-S1^{i} 97.58(8), S4-Fe1-S1^{i} 101.32(8). Symmetry transformation: ^{i} -x+1,-y+1,-z+1.

Previous studies carried out on various members of the electron transfer series $[Fe_2(dithiolene)_4]^n$ (n= from +1 to -2) combining DFT calculations with Mössbauer data support a +III oxidation state on both metal atoms independently of the dimer charge.[1i,10] To confirm this assignment in the case of compound **2**, its electronic structure was investigated by means of DFT calculations using the ADF program.[12] Calculations were performed on the experimental geometry (ESI). The spin density plot for complex **2**, represented in Figure **2**, shows three α and three β spins mainly located at the iron atoms. Two other unpaired electrons with α and β spins are respectively located on the two non-bridging terminal ligands and they are distributed among the sulfur, S3 and S4, and carbon, C1 and C2, atoms giving support to the radical character (S = 1/2) of the non-bridging ligands as inferred from the experimental bond lengths. The spin density for compound **2** constitutes the signature of an antiferromagnetic state.
To confirm theoretical predictions the magnetic properties of complex **2** were investigated.

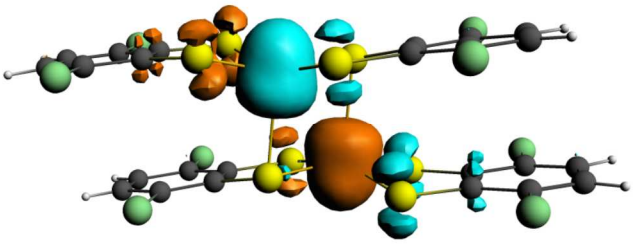

Figure 2. Representation of the BS-UDFT spin density (blue = α-spin; brown = β-spin) for compound **2**.

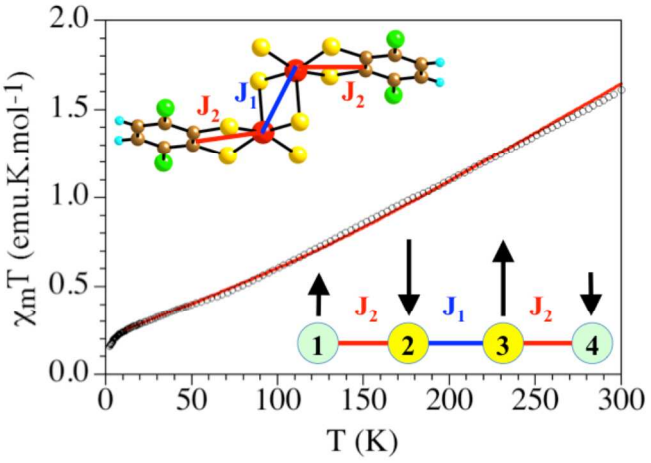

Figure 3. Thermal variation of the χ_mT product for compound **2**. Solid line is the best fit to the model.

The product of the magnetic susceptibility times the temperature, χ_mT for compound **2** shows a room temperature value of *ca*. 1.6 emu.K.mol^{-1} and a continuous decrease to reach a value of *ca*. 0.15 emu.K.mol^{-1} at 2 K (Figure 3). This behaviour indicates that compound **2** presents a strong antiferromagnetic coupling that is expected to arise from the coupling of the two Fe^{III} ions and the two S = 1/2 radicals. If we assume that the thienyl ligand is the terminal one, we obtain the magnetic exchange scheme depicted in the insets in Figure 3. Since the Fe^{III} atoms in dithiolene dimeric complexes can present a S = 3/2 or a S = 1/2 spin ground state,[9] we have tested both possibilities (ESI) in our fitting procedure by using the package MAGPACK.[13,14] The model using a S = 3/2 ground spin state for the Fe^{III} ions reproduces very satisfactorily the magnetic properties of compound **2** with the following parameters: g = 2.0 (fixed value), J_1 = –228 cm^{-1}, J_2 = –686 cm^{-1}, a temperature independent paramagnetism (Nα) of 3.0x10^{-4} emu-mol^{-1} and a monomeric Fe^{III} paramagnetic impurity of 1.0 % (solid line in Figure 3). To reduce the number of adjustable parameters we have fixed the g value to 2.0. This fit shows that the strongest AF interaction occurs between the Fe^{III} ions and the thienyl radicals through the direct double sulfur bridge (J_2) and that the Fe-Fe interaction through the double S bridge also leads to a strong AF coupling (J_1 = –228 cm^{-1}), in the range of those observed in other similar Fe^{III}-dithiolate dimers.[9] This result confirms the oxidation state +3 assumed for the Fe atoms in **2**. Note that the very strong J_2 coupling indicates the presence of a strong orbital overlap between the Fe(III) ion and the S atoms of the thienyl radical, in agreement with the planarity of the thienyl radical and the relatively small deviation of the Fe(III) atom from the basal plane. These two strong couplings give rise to the spin orientation indicated in inset in Figure 3, where the S = 3/2 spins are antiparallel as well as the two S = 1/2 of the thienyl radicals. This spin distribution leads to a total S = 0 ground spin state for the Fe^{III} dimer, in agreement with the magnetic properties and with the theoretical predictions.
Mössbauer studies also confirm the III+ oxidation state assignment for the metal atoms. Thus, the zero-field ^{57}Fe Mössbauer spectrum of complex **2** recorded at 77 K (Figure 4) shows a single doublet with isomer shift, δ = 0.345(2) mm/s, and quadrupole splitting, $|\Delta E_Q|$ = 2.94(1) mm/s, in agreement with theoretical calculation (δ = 0.378 mm/s, and quadrupole

splitting, $|\Delta E_Q| = 2.853$ mm/s) as well as the reported values for other Fe(III) square-pyramidal complexes.[1i,11]

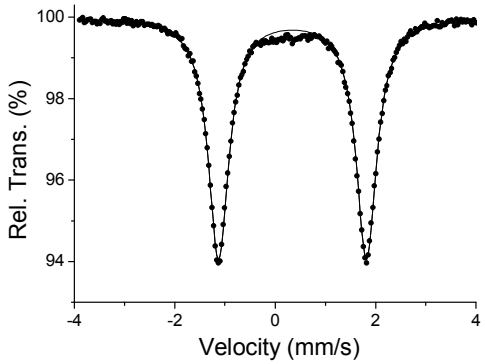

Figure 4. Mössbauer spectrum of compound **2** at 77 K.

Finally, we have to indicate that we were unable to study the electrochemical behaviour of compound **2** due to its insolubility in CH_2Cl_2 and instability in CH_3CN and thf solutions.

X-ray Diffraction, Mössbauer and Theoretical studies of Compound 3

The molecular structure of compound **3** is displayed in Figure 5. Selected bonds distances and angles are listed as figure caption (Figure 5). Taking into account the 18 electron rule compound $[Fe_3(CO)_7(\mu_3\text{-}SC_6H_2Cl_2S)_2]$ **3** is an electron precise 50 e^- cluster.

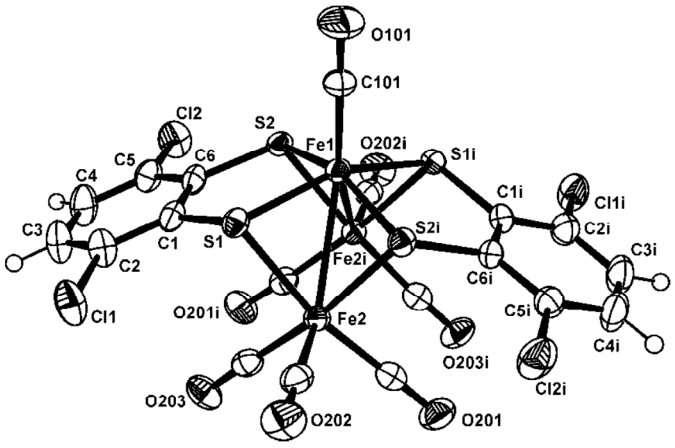

Figure 5. Molecular structure of **3**. Selected bond lengths (Å) and angles (deg): C1-C6 1.403(7), C1-S1 1.778(5), C6-S2 1.778(5), Fe1-Fe2 2.715(2), Fe2-Fe2^i 3.22(1), S1-Fe1 2.208(2), S2-Fe1 2.196(1), S1-Fe2 2.305(2), S2-Fe2^i 2.310(2), Fe2-Fe1-Fe2^i 72.71(5), Fe1-S1-Fe2 73.93(5), Fe1-S2-Fe2^i 74.05(5), S1-Fe1-S2 91.23(5). Symmetry transformation: ^{i} x,-y+1,-z+1.

The central heptacoordinated Fe(1) iron atom exhibits a distorted capped trigonal prism geometry, while the two external Fe(2) iron atoms are coordinated to the central Fe(1) atom, three carbonyl ligands and two sulfur atoms to complete a distorted octahedral geometry. A C_2 axis through the Fe1-C101-O101 unit makes equal both Fe(1)-Fe(2) bond distances, with a value of 2.715(2) Å. This interatomic distance is consistent with the presence of a metal-metal bond. However a non-bonding distance of 3.22(1) Å is observed between Fe(2)···Fe(2i) centres. The three metal Fe atoms form a bent triangular cluster with a Fe(2)-Fe(1)-Fe(2i) bond angle of 72.71 (5)º. This feature contrasts with the Fe(2)-Fe(1)-Fe(2) angle of 178.7(1)º found in the linear compound $[Fe_3(CO)_7(\mu_3\text{-}SC_6H_4N{=}N)_2]$[5] and the reported of 151.8(1)º and 156.22(4)º for the quasi-linear clusters $[Fe_3(CO)_7(\mu\text{-}SCH_2CH_2S)_2]$[3,7] (compound **4**) and $[Fe_3(CO)_7(\mu\text{-}SCH_2CH_2CH_2S)_2]$,[15] respectively. The internal iron atom is linked to a terminal CO ligand [O(101)-C(101)-Fe(1) angle of 180.0(4)º]. This is in contrast with the semi-bridging coordination mode observed for the CO ligand in the related $[Fe_3(CO)_7(SRS)_2$ (R=CH_2CH_2[3,7] and $CH_2CH_2CH_2$[15]] compounds. Additionally, in compound **3** each dithiolato group acts as a triple bridging ligand. Although two isomers (*syn* and *anti*) could be expected depending upon the orientation of the dithiolato groups, only the *syn* isomer has been observed for **3**. In contrast, the *anti*-isomer is observed in compounds $[Fe_3(CO)_7(\mu\text{-}SCH_2CH_2S)_2]$,[3,7] $[Fe_3(CO)_7(\mu\text{-}SCH_2CH_2CH_2S)_2]$[15] and $[Fe_3(CO)_7(\mu_3\text{-}SC_6H_4N{=}N)_2]$,[5] while in the case of the analogous ruthenium cluster $[Ru_3(CO)_7(\mu\text{-}SCH_2CH_2S)_2]$ both isomers have been isolated, although the *anti*-isomer is the most abundant.[4] Slight differences are observed in the mean central Fe-S and outer Fe-S bond distances in compounds $[Fe_3(CO)_7(\mu\text{-}SCH_2CH_2S)_2]$ **4**[3,7] and $[Fe_3(CO)_7(\mu\text{-}SCH_2CH_2CH_2S)_2]$.[15] However, the four bond distances between the sulfur atoms and the internal iron atom [S(1)-Fe(1) of 2.208(2) Å and S(2)-Fe(1) of 2.196(1) Å] are shorter than the corresponding bond lengths between the sulfur and the external iron atoms [S(1)-Fe(2) of 2.305(2) Å and S(2)-Fe(2i) of 2.310(2) Å]. These differences can be attributed to the triply bridging mode of the dithiolene ligand in **3** which forces a bent Fe-Fe-Fe structure and a lengthening of the Fe-Fe bond.

As far as we known, the crystal structures of compounds $[Fe_3(CO)_7(\mu\text{-}SCH_2CH_2S)_2]$,[3,7] $[Fe_3(CO)_7(\mu\text{-}SCH_2CH_2CH2S)_2]$,[15] $[Ru_3(CO)_7(\mu\text{-}SCH_2CH_2S)_2]$,[4] $[Mn_3(CO)_6(\mu\text{-}SCH_2CH_2CH_2S)_3]$[16] and $[Os_3(CO)_{10}(\mu\text{-}SCH_2CH_2S)]$,[17] are the only examples reported on transition metal carbonyl trinuclear clusters, containing dithiolato ligands. It is noteworthy that compound **3** exhibits some remarkable differences with those clusters: *i*) it represents the first example of this type of clusters containing aromatic instead aliphatic dithiolato ligands and *ii*) a triple bridging coordination mode is observed for the $-SC_6H_2Cl_2S-$ ligand, while the aliphatic dithiolato groups bridge two metals in the precedent examples. We have prepared the reported trinuclear cluster $[Fe_3(CO)_7(\mu\text{-}SCH_2CH_2S)_2]$ **4**[3,7] in order to carried out comparative studies with the new cluster $[Fe_3(CO)_7(\mu_3\text{-}SC_6H_2Cl_2S)_2]$ **3**. Additionally, they have been extended to the dinuclear derivative $[Fe_2(CO)_6(\mu\text{-}SC_6H_2Cl_2S)]$ **1**.[2] DFT studies of the three compounds have carried out at the OPBE level.[18] These complexes possess a singlet ground state in agreement with its diamagnetic nature. The experimental geometries are well reproduced by gas-phase geometry optimizations (Tables S1, S2 and Figure S1). In agreement with the before commented, the metal-metal distance in **3** is *ca.* 0.2 and 0.15 Å longer than those in compounds **1** and **4**, respectively. On the other hand, the optimized Fe(1)-S bond distances in compound **3** are *ca.* 0.15 Å shorter than the distances between the external Fe(2) atoms and their bonded sulfur atoms and the same tendency is also calculated for compound **4**. Although a mixed valence $Fe^IFe^{II}Fe^I$ state have been reported for $[Fe_3(CO)_7(SRS)_2$ (R=CH_2CH_2[3,7] and $CH_2CH_2CH_2$[15])] compounds in which each dithiolato is bridging two iron metals, the presence of two triple bridging "$SC_6H_2Cl_2S$"groups in cluster **3**, may also yields to another mixed valence possibilities such as $Fe^{II}Fe^0Fe^{II}$. In order to gain insight a Mössbauer experiment has been carried out on

compound **3.** The complexity associated with the isomer shift-oxidation state correlation in organometallic complexes, that can be explained on back-donation introduced by certain ligands which increase the electron density at the nuclei,[19,20] prompted us to extend the spectroscopic study to compounds **1** and **4** so similar coordination environments could be compared. (Figure 6, Table 1).

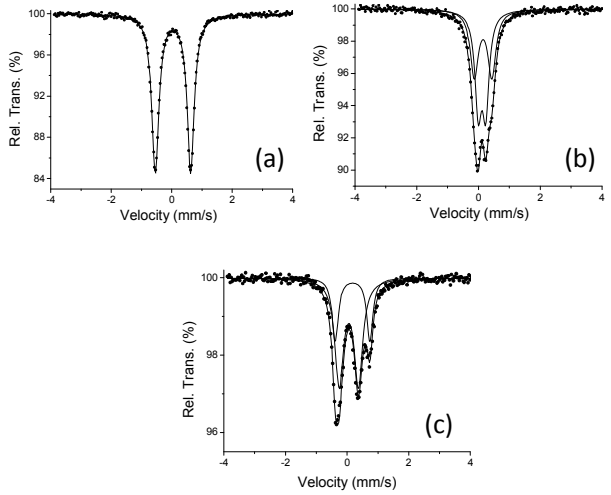

Figure 6. Mössbauer spectra of compounds **1** (a), **3** (b) and **4** (c) recorded at 77 K.

The spectrum of compound **3** (Figure 6b) results from the convolution of two quadrupole doublets, one with an area almost twice the other confirming the presence of two of the three iron atoms in a similar environment indicating a mixed valence states. Although a similar spectrum has been recorded for cluster $[Fe_3(CO)_7(\mu\text{-}SCH_2CH_2S)_2]$ **4**, different isomer shift values have been found for both clusters (Figure 6c, Table 1). On the other hand, as can see in Figure 6a, compound $[Fe_2(CO)_6(\mu\text{-}SC_6H_2Cl_2S)]$ **1** shows a single quadrupole doublet with an isomer shift value of δ = 0.058 mm/s at 77 K that is similar to the found at the same temperature for the outer iron atoms in compound $[Fe_3(CO)_7(\mu\text{-}SCH_2CH_2S)_2]$ **4** (δ = 0.046 mm/s). These data are consistent with a +I oxidation state,[6d,19] while values of δ = 0.116(1) and 0.156 (2) mm/s were found for cluster $[Fe_3(CO)_7(\mu_3\text{-}SC_6H_2Cl_2S)_2]$ **3**. This fact could indicate that compound **3** shows different iron oxidation states to those reported for **4**. On the other hand, analogous behaviour has been reported for the Fe^IFe^I compound $[Fe_2\{\mu\text{-}SCH_2C(CH_3)_2CH_2S\}(PMe_3)_2(CO)_4]$ (δ = 0.06 mm/s) and its oxidised specie Fe^IFe^{II} $[Fe_2(\mu\text{-}CO)\{\mu\text{-}SCH_2C(CH_3)_2CH_2S\}(PMe_3)_2(CO)_3]PF_6$ (δ = 0.105 and 0.190 mm/s).[20] Therefore, the above mentioned data do not allow us to assign the formal oxidation state, $Fe^IFe^{II}Fe^I$ or $Fe^{II}Fe^0Fe^{II}$, for compound **3**.

Mössbauer experimental parameters have been calculated for compounds **1**, **3** and **4** starting from their computed electronic structures and the results are listed in Table 1 together with the experimental values. The OPBE/TZP energies, $<S^2>$ values and electron density at the Fe nucleus ($\rho(0)$) employed for the calculation of Mössbauer isomer shift are given as ESI (Table S3). A good agreement between the experimental and calculated data is observed.

Table 1. Hyperfine parameters from the ^{57}Fe Mössbauer spectra for compounds **1**, **3** and **4** taken[a] at different temperatures T and DFT calculated[b] values at 0 K.

Compound	T (K)	δ(mm/s)	ΔE_Q (mm/s)	I
1[a]	295	-0.040 (2)	1.128(4)	100%
	77	0.058(1)	1.170 (1)	100%
1[b]	0	0.130	1.042	100%
3[a]	295	0.041(2)	0.261(7)	60%
		0.072 (3)	0.59(1)	40%
	77	0.116(1)	0.265(4)	65%
		0.156 (2)	0.593(8)	35%
3[b]	0	0.182	0.215	66%
		0.240	0.614	33%
4[a]	295	-0.010(6)	0.614(9)	66%
		0.100(7)	1.12(1)	33%
	77	0.046(1)	0.624(2)	63%
		0.176(2)	1.112(2)	37%
4[b]	0	0.117	0.640	66%
		0.274	1.047	33%

[a] IS isomer shift relative to metallic α-Fe at room temperature (mm/s); [b]Using the OPBE/TZP method.

Electrochemistry of Compound 3

The electrochemical behaviour of the trimetallic cluster $[Fe_3(CO)_7(\mu_3\text{-}SC_6H_2Cl_2S)_2]$ **3** was examined by cyclic voltammetry (CV) in dichloromethane using $[n\text{-}Bu_4N][PF_6]$), as supporting electrolyte.

When the potential is scanned in the cathodic direction, from 0 to –2.0 V region, cluster **3** shows a reduction process at E_{pc} = –0.69 V, *vs* SCE (Figure 7).

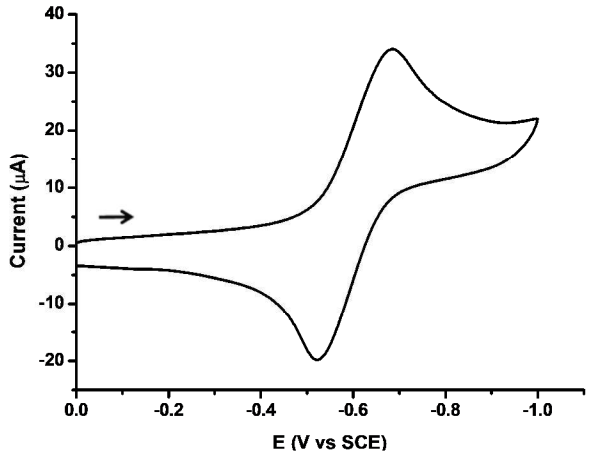

Figure 7. Cyclic voltammetric response, on glassy-carbon working electrode at a scan rate of 0.1 V s^{-1}, of trinuclear cluster $[Fe_3(CO)_7(\mu_3\text{-}SC_6H_2Cl_2S)_2]$ (**3**) recorded in CH_2Cl_2 containing 0.1 M $[n\text{-}Bu_4N][PF_6]$.

For this redox couple, the plot of peak current (i_p) versus $v^{1/2}$ was linear, indicating that redox process was diffusion controlled. Likewise, the voltammetric features (i_{pc}/i_{pa} essentially equal to unity, ΔE_p values about 85–100 mV at slow scan rates, and E_p independent of v) show that the reduction of compound **3** is chemically reversible on the voltammetric time scale.[21] The number of electrons transferred in the redox

process was estimated by cyclic voltammetry, by comparison of the current intensity of the CV of **3** with that of an equimolar amount of decamethylferrocene (Cp^*_2Fe)[22] (Figure S2). This established that the cathodic couple of **3** involves the transfer of one electron, and suggests the formation of the monoanionic species $[Fe_3(CO)_7(\mu_3\text{-}SC_6H_2Cl_2S)_2]^-$. A simplistic analysis of the frontier orbitals in **3** (Figure 8) suggest that the electron enters a LUMO orbital which is basically formed by the d_z^2 orbitals of the external iron atoms. This fact could indicated that the higher oxidation state is located on them.

In contrast, the reduction process reported for complex **4** is irreversible and shows a cathodic shift of *ca*. 300 mV with regard to that of compound **3**.[7] A frontier orbital analysis on **4** (Figure S3) indicates that upon reduction the entering electron occupies an Fe-Fe antibonding orbital. For comparison, the redox behaviour of the related di-iron compound $[Fe_2(CO)_6(\mu\text{-}S_2C_6H_2Cl_2)]$ **1** has been investigated (Figure S4). This bimetallic compound undergoes a single reversible diffusion-controlled reduction at –0.90 V *vs* SCE, which also shows cathodic shift with respect to the first reduction peak of **3** (–0.69 V). Consequently, the reduction of trimetallic compound **3** is thermodynamically easier than that of compounds **1** and **4**.

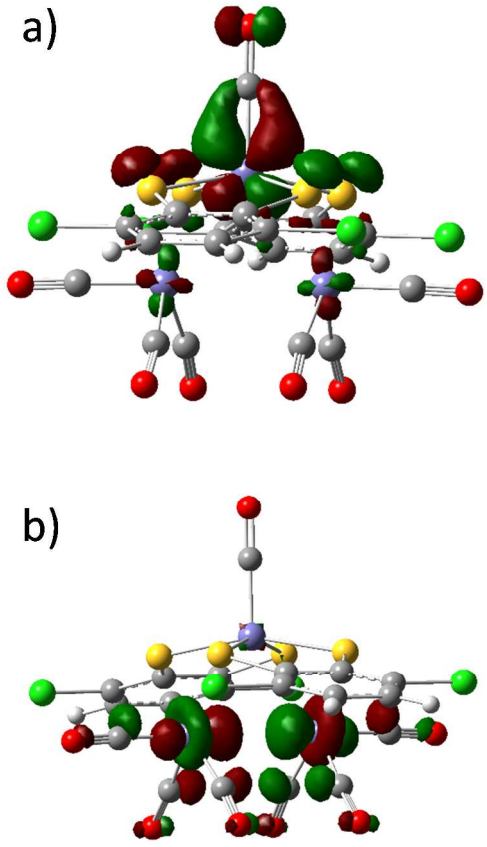

Figure 8. VP-2 representation of HOMO (a) and LUMO (b) orbitals of compound **3** calculated using DFT.

In the anodic region, tri-iron cluster **3** exhibits a quasi-reversible oxidation wave (Figure S5), whose current intensity closely approximates to that of the reduction process described above. Therefore, the oxidation peak at +1.11 V *vs* SCE could be attributed to a one-electron oxidation process. Based on the frontier orbital analysis the electron is removed from an orbital which has a major contribution from the π^* C-O orbital and a minor contribution from the d_{yz} orbital of inner Fe atom.

Additionally, the ability of $[Fe_3(CO)_7(\mu_3\text{-}SC_6H_2Cl_2S)_2]$ **3** to act as electrocatalyst for proton reduction to H_2 has been evaluated. Figure 9 provides CV responses of **3** in 0.1 M CH_2Cl_2/[*n*-Bu_4N][PF_6], obtained in the absence and presence of $HBF_4{\cdot}OEt_2$. As can be observed, when the first 3 equivalents of $HBF_4{\cdot}OEt_2$ acid were added, the reduction peak of **3** considerably increased and continued to grow in intensity with sequential addition of the acid. When 15 equivalents of acid were added, the reduction peak reaches a maximum height, which is about seven times higher than the original reduction of **3**, in the absence of acid. At this point, when the potential scan direction is reversed, no complementary oxidation peak is observed. This behaviour is typical for a fast irreversible chemical reaction coupled to the charge-transfer step. The rapid increment in current height of the reduction peak in the presence of acid suggests an electrocatalytic process.[23] The obtained result qualitatively resembles to that of related thiolate derivatives previously described by Hogarth and col.[7] and by Pickett and col.[8] containing tri-iron and tetra-iron assemblies, respectively.

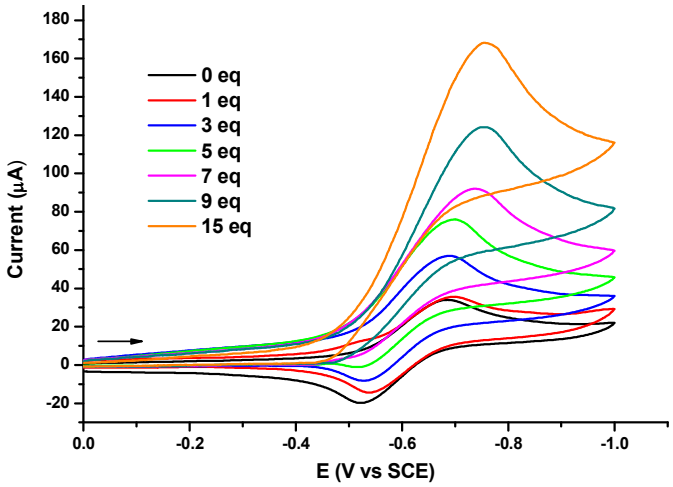

Figure 9. Cyclic voltammetric response of compound **3** (10^{-3} M) measured in CH_2Cl_2 containing 0.1 M [*n*-Bu_4N][PF_6] in the absence (black line) and in the presence (colour lines) of increasing amounts of $HBF_4{\cdot}OEt_2$ acid.

Experimental

General. All reactions were carried out under argon atmosphere. Solvents were dried using standard methods. $Fe_3(CO)_{12}$ and 1,2-dithiol $HSC_6H_2Cl_2SH$ are commercially available (Aldrich). $[Fe_2(CO)_6(\mu\text{-}SC_6H_2Cl_2S)]$[2] and $[Fe_3(CO)_7(\mu\text{-}SCH_2CH_2S)_2]$[3] were prepared according to the published procedure. The infrared spectra were recorded on a Perkin-Elmer Spectrum BX FT-IR spectrophotometer using NaCl cells. ^{1}H NMR spectra were registered on a Bruker AMX-300 instrument. Elemental analyses were performed on an LECO CHNS-932 Elemental Analyzer. FAB or MALDI-TOF mass spectra were carried out on a WG Autospec Spectrometer or ULTRAFLEX III using 3-nitrobenzyl alcohol or DCTB as matrix, respectively.

Reaction of $[Fe_2(CO)_6(\mu\text{-}SC_6H_2Cl_2S)]$ 1 with $HSC_6H_2Cl_2SH$. A mixture of $[Fe_2(CO)_6(\mu\text{-}SC_6H_2Cl_2S)]$ (200 mg, 0.41 mmol) and $HSC_6H_2Cl_2SH$ (260 mg, 1.23 mmol) in toluene (15 mL), was refluxed during 24 h. Afterwards, the dark solid formed in

the reaction, was filtered and recrystallized in wet acetone/n-hexane (1:2) at –20 ºC, yielding compound $[Fe_2(SC_6H_2Cl_2S)_4]$ **2** (27 mg, 6.9 %). MS (MALDI-TOF): *m/z* 947.5 $[Fe_2(SC_6H_2Cl_2S)_4]^-$, 473.8 $[Fe(SC_6H_2Cl_2S)_2]^-$. Anal. Calcd. for $C_{24}H_8Cl_8Fe_2S_8.4H_2O{\cdot}C_3H_6O$; C, 30.07; H, 2.04; S, 23.76. Found: C, 29.08; H, 1.99; S, 24.12.

Reaction of $Fe_3(CO)_{12}$ with $HSC_6H_2Cl_2SH$. To a solution of $Fe_3(CO)_{12}$ (300 mg, 0.60 mmol) in toluene (15 mL), $HSC_6H_2Cl_2SH$ (250 mg, 1.19 mmol) was added. The resulting mixture was kept under stirring at 110 ºC for 3 h. The colour of the mixture changed from deep green to brown-red. The solvent was removed under reduced pressure, and the residue purified by chromatographic column on silica gel. Elution with n-hexane gave a major first band of $[Fe_2(CO)_6(\mu\text{-}SC_6H_2Cl_2S)]$ **1** (180 mg, 63 %). A second band, eluted with CH_2Cl_2 gave the brown compound $[Fe_3(CO)_7(\mu_3\text{-}SC_6H_2Cl_2S)_2]$ **3** (30 mg, 6.4 %). Elution with wet acetone yields the purple compound $[Fe_2(SC_6H_2Cl_2S)_4]$ **2** (95 mg, 17.3 %).

Single crystals of **3** were obtained from CH_2Cl_2/n-hexane (1:4) at –20 °C. Spectroscopic data for compound **3**: IR (hexane): υ_{CO} (cm^{-1}) 2077 (m), 2054 (vs), 2022 (w), 2016 (s), 1999 (vw), 1977 (s). ^1H NMR ($CDCl_3$, 300 MHz, 22 ºC) δ 7.10 ppm (s, 4H, C_6H_2). MS (FAB): *m/z* 781.5 $[M^+]$, 753.5-613.5 $[M^+$-nCO, n=1-6]. Anal. Calcd. for $C_{19}H_4Cl_4O_7S_4Fe_3{\cdot}2CH_2Cl_2$; C, 26.48; H, 0.84; S, 13.45. Found: C, 26.51; H, 0.79; S, 13.11.

Reactivity of $Fe_3(CO)_{12}$ with $HSC_6H_2Cl_2SH$ in the presence of $ONMe_3$. To a thf (15 mL) solution of $Fe_3(CO)_{12}$ (150 mg, 0.3 mmol), $ONMe_3$ (166 mg, 1.5 mmol) and $HSC_6H_2Cl_2SH$ (126 mg, 0.6 mmol) were added. The resulting mixture was stirred at room temperature for 20 min. Afterwards the green colour of the solution changed to brown. Then, the solvent was removed under reduced pressure and the residue purified by chromatographic column on silica gel. Elution with n-hexane gave a red band of $[Fe_2(CO)_6(\mu\text{-}SC_6H_2Cl_2S)]$ **1** (11 mg, 7.7%) followed by a second brown band corresponding to compound $[Fe_3(CO)_7(\mu_3\text{-}SC_6H_2Cl_2S)_2]$ **3** (traces amount) using CH_2Cl_2 as eluent. Finally, a third purple band went down from the column using wet acetone to yield compound $[Fe_2(SC_6H_2Cl_2S)_4]$ **2** (115 mg, 40 %).

Mössbauer Studies. Mössbauer spectra were carried out at 293 K and 77 K in triangle mode using a conventional spectrometer with ^{57}Co(Rh) source. The spectra were analysed by a nonlinear fit using the NORMOS program[24] and the energy calibration was made using a α-Fe (6 μm) foil.

Magnetic Measurements. Variable temperature susceptibility measurements were carried out in the temperature range 2-300 K with an applied magnetic field of 0.1 T on ground polycrystalline samples of compound **2** (with masses of 13.79), with a Quantum Design MPMS XL-5 SQUID magnetometer. The susceptibility data were corrected for the sample holders previously measured under the same conditions and for the diamagnetic contributions of the sample using Pascal´s constants tables.[25]

Electrochemical Measurements. Cyclic voltammetric (CV) experiments were recorded on a Bioanalytical Systems BASCV-50W potentiostat. CH_2Cl_2 (SDS, spectrograde) for electrochemical measurements was freshly distilled from calcium hydride under argon. The supporting electrolyte used was a 0.1 M solution of tetra-*n*-butylammonium hexafluorophosphate (Fluka), which was purified by recrystallization from ethanol and dried in vacuum at 60 °C. A conventional three-electrode cell connected to an atmosphere of prepurified nitrogen was used. All cyclic voltammetric experiments were performed using either a platinum-disk working electrode (A = 0.020 cm^2) or a glassy carbon-disk working electrode (A = 0.070 cm^2) (both Bioanalytical Systems), each of which was polished on a Buehler polishing cloth with Metadi II diamond paste, rinsed thoroughly with purified water and acetone, and dried. All potentials were referenced to the saturated calomel electrode (SCE). Under our conditions, the ferrocene redox couple $[FeCp_2]^{0/+}$ is +0.462, and decamethylferrocene redox couple $[FeCp^*_2]^{0/+}$ is –0.056 V vs SCE in CH_2Cl_2/0.1 M n-Bu_4NPF_6. A coiled platinum wire was used as a counter electrode. Solutions were, typically, 10^{-3} M in the redox active species.

X-ray Structure Analysis of 2 and 3. Crystals were removed from the Schlenk and covered with a layer of a viscous perfluoropolyether (Fomblin®Y). A suitable crystal was selected with the aid of a microscope, attached to a glass fiber, and immediately placed in the low temperature nitrogen stream of the diffractometer. The intensity data sets were collected at 200 K on a Bruker-Nonius KappaCCD diffractometer equipped with an Oxford Cryostream 700 unit. The structures were solved, using the WINGX package,[26] by direct methods (SHELXS-97) and refined by least-squares against F^2 (SHELXL-97).[27] Complex **2** crystallized with four water molecules and one of acetone. Due to the poor quality of the crystal, all of them presented severe disorder and it was not possible to define a sensible chemical model, so Squeeze[28] procedure was performed to remove their contribution to the structure factors. All the hydrogen atoms in both structures were positioned geometrically and refined by using a riding model while all non-hydrogen atoms were anisotropically refined.

Computational Methods. All calculations were carried out using DFT methodology in combination with all-electron Slater-type triple-ζ plus polarization (TZP) basis set as implemented in the ADF program.[12] The OPBE functional is recommended for the calculation of Mössbauer spectroscopy and, therefore, it is employed on all calculations.[18] Compounds **1** and **3** were calculated using the restricted formalism and geometrically optimized while for compound **2** the broken-symmetry unrestricted technique was employed to find the antiferromagnetic state using the X-ray structure geometry. Relatistic effects were considered except for the calculation of isommer shifts. In order to use the Noodleman fitting values the same options must be used, then relativistic effects were omitted and integration grid was lowered to 5.5.[29]

Conclusions

The reaction between $Fe_3(CO)_{12}$ and $HSC_6H_2Cl_2SH$ has been revisited. In addition to the already reported $[Fe_2(CO)_6(\mu\text{-}SC_6H_2Cl_2S)]$ **1** product, two new iron complexes, $[Fe_2(SC_6H_2Cl_2S)_4]$ **2** and $[Fe_3(CO)_7(\mu_3\text{-}SC_6H_2Cl_2S)_2]$ **3** have been isolated. In the course of the reaction cluster **3** is converted into **2** towards the known compound **1**.

X-ray crystallography, Mössbauer spectroscopy and theoretical calculations have allowed unequivocally to assign the oxidation state +III for the iron metals in compound **2**. Magnetic measurements confirm a strong antiferromagnetic coupling and its magnetic moment arises from the coupling of two Fe^{III} ions (S= 3/2) and two S= 1/2 radicals, in agreement with the DFT calculated spin electronic density for this compound.

The crystal structure of **3** shows two dithiolato ligands in an unusual triple bridging coordination mode and also represents the first example among the few related carbonyl trinuclear

clusters of the group 8 metals, which contains an aromatic dithiolato ligand.

Mössbauer parameters for compounds **1**, **3** and **4** have been calculated from DFT computed electronic structures and there is a very good agreement between experimental and calculated values.

Cyclic voltammetric experiments on compound **3** show a reversible reduction peak corresponding to one electron. Additionally, electrochemical results suggest that compound that **3** can function, in the presence of acid, as a catalyst for proton reduction.

Mössbauer and theoretical data do not confirm the iron oxidation states in the mixed valence cluster $[Fe_3(CO)_7(\mu_3\text{-}SC_6H_2Cl_2S)_2]$ **3**.

Acknowledgements

Financial support from Spain's Ministerio de Economía y Competitividad (MINECO) (projects CTQ2011-23157, CTQ2011-26507, CTQ2012-30728, MAT2010-20843-C02-01 and MAT2012-37109-C02-02), Generalitat Valenciana (Project Prometeo 2009/95 ISIC and ACOMP/2013/215) and Factoria de Cristalización (CONSOLIDER-INGENIO 2010) is gratefully acknowledged. We thank Dr. Popescu for useful discussion on Mössbauer studies.

Notes and references

[a] Departamento de Química Inorgánica, Universidad Autónoma de Madrid, 28049 Madrid, Spain. [b] Instituto de Ciencia Molecular, 46980 Paterna, Valencia, Spain. [c] Departamento de Química Física y Analítica, Universidad de Castellón, 12071 Castellón de la Plana, Spain. [d] Departamento de Química Orgánica y Química Inorgánica, Universidad de Alcalá de Henares, 28871, Alcalá de Henares, Spain. [e] Departamento de Química Física Aplicada, Universidad Autónoma de Madrid, 28049 Madrid, Spain. [f] Departamento de Química Física. Universidad de Zaragoza e Instituto de Biocomputación y Física de Sistemas Complejos (BIFI), 50009 Zaragoza, Spain. [g] CSIC, Insituto de Química Física Rocasolano, 28006, Madrid, Spain.

Electronic Supplementary Information (ESI) available: CCDC reference numbers 1002771 (**2**), 1002772 (**3**) as well as additional experimental and theoretical data. See DOI: 10.1039/b000000x.

Dedicated to Professor David Cole-Hamilton on the occasion of his retirement and for his outstanding contribution to transition metal catalysis.

1. (a) Robertson, N.; Cronin, L. *Coord. Chem. Rev.* **2002**, *227*, 93-127. (b) *Progress in Inorganic Chemistry,* vol. 52, Dithiolene Chemistry: Synthesis, Properties, and Applications, Eds. Karlin, K. D.; Stiefel, E. I. John Wiley and Sons, New York, **2004**. (c) Muller-Westerhoff, U. T.; Vance, B. in *Comprehensive Coordination Chemistry*, Eds. Wilkinson, G.; Gillard, R. D., McCleverty J. A. Pergamon Press, Oxford, 1nd. Edn. **1987**, vol. 2. (d) Clemenson, P. I. *Coord. Chem. Rev.* **1990**, *106*, 171-203. (e) Belo, D.; Almeida, M. *Coord. Chem. Rev.* **2010**, *254*, 1479-1492. (f) Ezzaher, S.; Gogoll, A.; Bruhn, C.; Ott S. *Chem. Commun.* **2010**, 5775-5777, and references herein. (g) Alcácer, L.; Novais, H. in *Extended Linear Chain Compounds,* Ed. Miller, J. S. Plenum Press, New York **1983**. (h) Cassoux, P.; Valade, L.; Kobayashi, H.; Kobayashi, A.; Clark, R. A.; Underhill, A. E. *Coord. Chem. Rev.* **1991**, *110*, 115-160. (i) Sproules, S.; Wieghardt, K. *Coord. Chem. Rev.* **2010**, *254,* 1358-1382.

2. Schwartz, L.; Singh, P. S.; Eriksson, L.; Lomoth, R.; Ott, S. *C.R. Chimie* **2008**, *11*, 875-889.

3. Winter, A.; Zsolnai, L.; Huttner, G. *Z. Naturforsch* **1982,** *37b*, 1430-1436.

4. Adams, R. D.; Yamamoto, J. H. *J. Cluster. Sci.* **1996**, *7,* 643-654.

5. Pannell, K. H.; Mayr, A. J.; Van Derveer, D. *J. Am. Chem. Soc.* **1983**, *105*, 6186-6188.

6. (a) Streich, D.; Karnahl, M.; Astuti, Y.; Cady, C. W.; Hammarrstrom, L.; Lomoth, R.; Ott, S. *Eur. J. Inorg. Chem*. **2011**, 1106-1111, and references therein. (b) Wright, R. J.; Lim, C.; Tilley, T. D. *Chem. Eur. J.* **2009**, *15*, 8518-8525. (c) Durgaprasad, G.; Bolligarla, R.; Das, S. K. *J. Organomet. Chem*. **2012**, *706-707*, 37-45. (d) Apfel, U. P.; Troegel, D.; Halpin, Y.; Tschierlei, S.; Uhlemann, U.; Georls, H.; Schmitt, M.; Popp, J.; Dunne, P.; Venkatesan, M.; Coey, M.; Rudolph, M.; Vos, J. G.; Tacke, R.; Weigand, W. *Inorg. Chem.* **2010**, *49*, 10117-10132. (e) Tard, C.; Pickett, C. J. *Chem. Rev*. **2009**, *109*, 2245-2274.

7. Ghosh, S.; Hogarth, G.; Holt, K. B.; Kabir, S. E.; Rahaman, A.; Unwin, D. G. *Chem. Commun.* **2011**, 11222-11224.

8. Tard, C.; Liu, X.; Hughes, D. L.; Pickett, C. J. *Chem. Commun*. **2005**, 133-135.

9. Amo-Ochoa, P.; Delgado, E.; Gómez-García, C. J.; Hernández, D.; Hernández, E.; Martin, A.; Zamora, F. *Inorg. Chem*. **2013**, *52*, 5943-5950.

10. Patra, A. K.; Bill, E.; Weyhermüller, T.; Stobie, K.; Bell, Z.; Ward, M. D.; McCleverty, J. A.; Wieghardt, K. *Inorg. Chem*. **2006**, *45*, 6541-6548.

11. Yu, R.; Arumugam, K.; Manepalli, A.; Tran, Y.; Schmehl, R.; Jacobsen, H.; Donahue, J. P. *Inorg. Chem*. **2007**, *46*, 5131-5133.

12. (a) ADF2010.02; SCM, Theoretical Chemistry, Vrije Universiteit, Amsterdam, The Netherlands. (b) te Velde, G.; Bickelhaupt, F. M.; Baerends, E. J.; Fonseca Guerra, C.; Van Gisbergen, S. J. A.; Snijders, J. G.; Ziegler, T. *J. Comput. Chem*. 2001, 22, 931-967.

13. Borrás-Almenar, J. J.; Clemente-Juan, J. M.; Coronado, E.; Tsukerblat, B. S. *Inorg. Chem.* **1999**, *38*, 6081-6088.

14. Borrás-Almenar, J. J.; Clemente-Juan, J. M.; Coronado, E.; Tsukerblat, B. S. *J. Comput. Chem.* **2001**, *22*, 985-991.

15. Hu, M.; Ma, C.; Wen, H.; Cui, H.; Chen, C. *Acta Cryst.* **2014**, *E70*, m124.

16. Begum, N.; Hyder, M. I.; Kabir, S. E.; Hossain, G. M. G.; Nordlander, E.; Rokhsana, D.; Rosenberg, E. *Inorg. Chem.* **2005**, *44*, 9887-9894.

17. Adams, R. D.; Chen, L.; Yamamoto, J. H. *Inorg. Chim. Acta* **1995**, *229,* 47-54.

18. (a) Handy, N. C.; Cohen, A. J. *Mol. Phys*. **2001**, *99*, 403-412. (b) Perdew, J. P.; Burke, K.; Ernzerhof, M. *Phys. Rev. Lett*. **1996**, *77*,

785-789. (c) Perdew, J. P.; Burke, K.; Ernzerhof, M. *Phys. Rev. Lett*. **1997**, *78*, 1396.

19 Hsieh, C-H.; Erdem, O. F.; Harmann, S. D.; Singleton, M. L.; Reijerse, E.; Lubitz, W.; Popescu, C. V.; Reibenspies, J. H.; Brothers, S. M.; Hall, M. B.; Darensbourg, M. Y. *J. Am. Chem. Soc*. **2012**, *134*, 13089-13102.

20. Stoian, S. A.; Hsieh, Ch.-H.; Singleton, M. L.; Casuras, A. F.; Darensbourg, M.Y.; McNeely, K.; Sweely, K.; Popescu, C. V. *J. Biol. Inorg. Chem.,* **2013**, *18*, 609-622.

21. Electrochemical Methods, Eds. Bard, A.J.; Faulkner, L.R. John Wiley & Sons, New York, **1980**.

22. Inorganic Electrochemistry. Theory, Practice and Application; 2nd Edition. Eds. Zanello, P.; Nervi, C.; Fabrizi de Biani, F. Royal Society of Chemistry, Cambridge, **2012**.

23. (a) Bhugun, I.; Lexa, D.; Saveant, J.-M. *J. Am. Chem. Soc.* **1996**, *118*, 3982-3983. (b) Borg, S. J.; Behrsing, T.; Best, S. P.; Razavet, M.; Liu, X.; Pickett, C. J. *J. Am. Chem. Soc*. **2004**, *126*, 16988-16999.

24. Brand, R. A. *Nucl. Inst. Meth. Phys. Res*. **1987**, *B28*, 398-416.

25. Bain, G. A.; Berry, J. F. *J. Chem. Educ.* **2008**, *85*, 532-536.

26. Farrugia, L. J. *J. Appl. Crystallogr.* **1999**, *32*, 837-838.

27. Sheldrick, G. M. *Acta Crystallogr. Sect. A* **2008**, *A64*, 112-122.

28. Van der Sluis, P.; Spek, A. L. *Acta Crystallogr. Sect. A* **1990**, *A46*, 194-201.

29. Sandala, G. M.; Hopmann, K. H.; Ghosh, A.; Noodleman, L. *J. Chem. Theor. Comput*. **2011**, *7*, 3232-3247.

Contents Entry:

The reaction of $Fe_3(CO)_{12}$ with $HSC_6H_2Cl_2SH$ gives the trinuclear cluster $[Fe_3(CO)_7(\mu_3\text{-}SC_6H_2Cl_2S)_2]$ **3** that evolves to the neutral iron dithiolate derivative $[Fe_2(SC_6H_2Cl_2S)_4]$ **2** *via* the intermediate compound $[Fe_2(CO)_6(\mu\text{-}SC_6H_2Cl_2S)]$ **1**. The cluster **3** consists of a mixed valence compound in which the dithiolato ligands show a triple bridging coordination mode. Compound **2** is a Fe^{III} dimer where a thiolate and a thienyl coordinate to each iron atoms.